G. Mahan, J. Chem. Phys. 52, 258 (1970).
[5]W. E. Baylis, Phys. Rev. A 1, 990 (1970).
[6]For related work in nonalkali systems see, for example, G. Ewing, Angew. Chem. 11, 486 (1972).
[7]W. E. Baylis, J. Chem. Phys. 51, 2665 (1969); corrected values by private communication.
[8]F. A. Franz and C. E. Sooriamoorthi, Phys. Rev. A 8, 2390 (1973), and 10, 126 (1974).
[9]M. Aymar, M. A. Bouchiat, and J. Brossel, J. Phys. (Paris) 30, 615 (1969).
[10]The accuracy of Eq. (2) has been estimated to be greater than 98%. The constant term 0.6 represents the value in the present experiment of the term $2B_3C_3 \times (B_2 - C_2)^{-1}$. See Ref. 8 for definitions and details.
[11]We have used the average of the values reported by F. Grossetete and J. Brossel, C. R. Acad. Sci. 264, 381 (1967), and H. M. Gibbs and R. J. Hull, Phys. Rev. 153, 132 (1967).
[12]*Zahlenwerte and Funktionen aus Physik, Chemie, Astronomie, Geophysik und Technik*, edited by K. Schäfer and E. Lax (Springer, Berlin, 1960), Vol. II, Pt. 2a, p. 12.
[13]F. A. Franz and C. Volk, to be published.
[14]C. P. Slichter, *Principles of Magnetic Resonance* (Harper and Row, New York, 1963), p. 141, Eq. (37).
[15]J. Vanier, J. F. Simard, and J. S. Boulanger, Phys. Rev. A 9, 1031 (1974).
[16]E. I. Dashevskaya and E. A. Kobzeba, Opt. Spectrosc. 30, 436 (1971).
[17]R. M. Herman, Phys. Rev. 136, A1576 (1964).

Localized Fields and Density Perturbations Due to Self-Focusing of Nonlinear Lower-Hybrid Waves*

W. Gekelman and R. L. Stenzel
Department of Physics, University of California, Los Angeles, California 90024
(Received 9 June 1975)

Large-amplitude lower-hybrid wave bursts at $\omega_0 > \omega_{LH}$ are excited from a grid and propagate into a density gradient perpendicular to $\vec{B}_0$. The evolution of the internal rf fields and the plasma parameters is investigated. Above threshold localized field maxima appear ($E_{int} \gg E_{appl}$) and, simultaneously, strong density perturbations are formed. The nonlinear phenomena are interpreted by ponderomotive-force and space-charge separation effects.

Nonlinear wave phenomena are a topic of strong current interest. The ponderomotive force in strong nonuniform rf fields can change the local plasma parameters which may enhance the field and lead to instabilities. Filamentation instabilities of plane waves have been discussed in the literature for both unmagnetized[1] and magnetized plasmas.[2] The present work is concerned with a filamentation process of an initially nonuniform rf field, i.e., the resonance cone pattern[3] associated with lower-hybrid waves. Locally growing density depressions and internal rf fields are observed.

The experiment is performed in a large (12 cm diam, 150 cm length), quiescent ($\delta n/n \simeq 1\%$), weakly collisional ($\nu_{en}/\omega < 10^{-2}$), magnetized ($B_0 \simeq 500$ G) plasma column ($n_e \simeq 10^{10}$ cm^{-3}, $T_e \sim 2$ eV) described in detail elsewhere.[4] In a previous experiment[5] we studied the three-dimensional propagation of small-amplitude lower-hybrid waves in the uniform center region of the column (~ 8 cm diam). By suitably modifying the cathode, we have now established a constant density gradient ($n/\nabla n \simeq 15$ cm over 8 cm across $\vec{B}_0$, see Fig. 1) and are able to launch waves from the low-density side with $\vec{k} \perp \nabla n$, $\vec{k} \perp \vec{B}_0$. The exciter grid is 66 cm long, 3.5 cm high, and consists of fourteen electrically connected, plane parallel to $\vec{B}_0$, spring-loaded, 0.1-mm-diam tungsten wires. With this design we minimize density perturbations yet establish an equipotential surface in the plasma, which closely matches the phase front of lower-hybrid normal modes. The waves are detected with T probes (3 cm length, 0.1 mm diam, 1-mm-o.d. coaxial feed), movable axially along $\vec{B}_0$ and in the radial directions (parallel and perpendicular to the exciter-grid surface normal, respectively). Phase-coherent wave bursts ($4 < f < 20$ MHz, $0.05 < t < 10$ μsec, $1 < V_0 < 60$ V peak to peak at $Z = 50$ Ω) are applied to the exciter grid. The received signals are analyzed with a sampling oscilloscope and/or boxcar integrator.

The propagation of lower-hybrid waves along a density gradient reveals a more complicated structure than in a uniform plasma. Figure 1 shows backward lower-hybrid waves near the exciter bounded by a standing wave corresponding

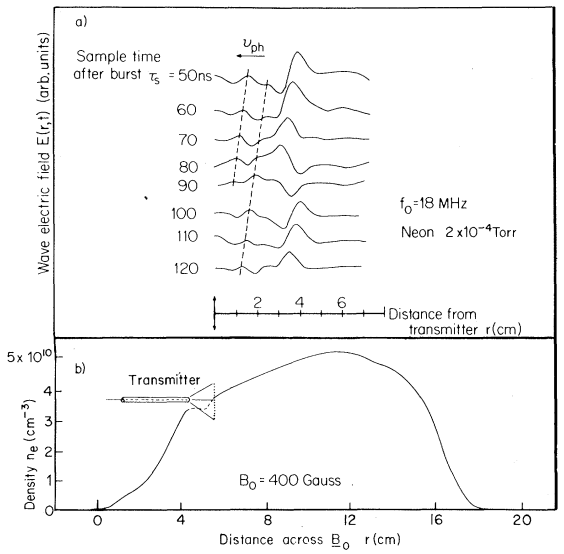

FIG. 1. (a) Wave electric field versus radial position perpendicular to $\vec{B}_0$ sampled at various times after turn-on of a small-amplitude tone burst [$\omega/(\omega_{LH})_{max} \simeq 3$]. Backward lower-hybrid waves bounded by a large-amplitude oscillation at the resonance cone are seen. Burst length, 500 nsec; repetition rate, 1 kHz. (b) Radial density profile with schematic view of lower-hybrid-wave exciter located at the foot of a long linear density gradient across $\vec{B}_0$.

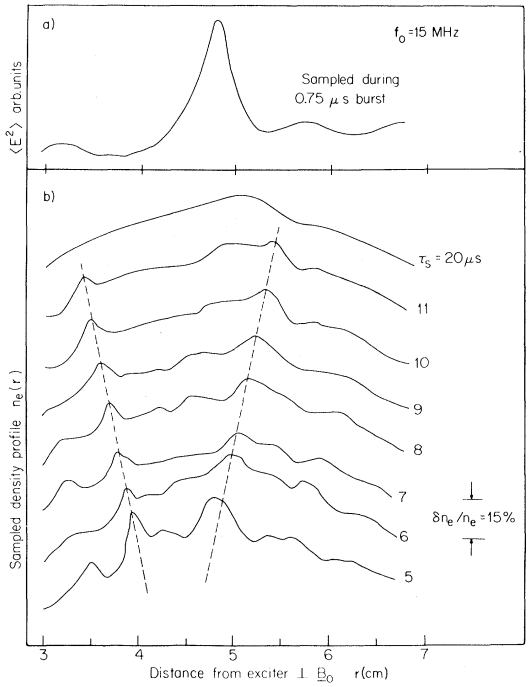

FIG. 2. (a) Time-averaged square of the electric field versus radial position in the nonlinear case, sampled during the final 250 nsec of the 750-nsec burst. Plasma density, B_0, and repetition rate are the same as in Fig. 1. (b) Sampled radial density profile (zero lines suppressed) at various times τ_s after the end of the exciter burst. The lowest curve ($\tau_s = 5$ μsec) indicates a density perturbation of 15%.

to the cone edge. The phase velocity is nearly perpendicular to $\vec{B}_0$; the group velocity is nearly parallel to the cone edge.[5] If the frequency is chosen close to the lower-hybrid resonance, the cone angle [$\tan^2\theta = k_\parallel{}^2/k_\perp{}^2 \simeq (\omega^2/\omega_{LH}{}^2 - 1)\, m_e/m_i$] is very small and the waves cannot penetrate deep into the plasma in a finite-length device. In order to study large-amplitude effects well separated from the exciter grid, we have chosen a frequency higher than the maximum lower-hybrid frequency [$\omega \gtrsim 3(\omega_{LH})_{max}$] so as to obtain $\theta > 2°$. Then there are only a few wavelengths in the column across $\vec{B}_0$ as shown in Fig. 1.

As the amplitude of the applied rf burst is increased, two nonlinear effects are observed: modifications of the density profile and evolution of new sharp peaks of the internal rf fields. Figure 2 gives an example of the large-amplitude rf field distribution in the column (top trace) and the modified density profile at different times after the end of the rf burst (bottom traces). The rf burst length of 750 nsec is short enough to avoid collisional heating and ionization.

The electric field is measured with a double T probe (1 mm spacing of parallel wires) by subtracting the signals of each probe with a hybrid tee. The probe is calibrated in known field geometries in vacuum (parallel plates, coaxial cylinders) after verifying that it responds to electric fields rather than to rf potentials as the single T probe does.

Figure 3 shows both the applied rf amplitude (top traces) and the internal rf field (bottom traces) versus time at different applied rf powers with the probe located on the resonance cone. The measured local rf field is as large as 30 V/cm for an applied field of $E_{appl} \simeq 1.5$ V/cm. This enhancement is partly due to the linear resonant enhancement and partly due to an instability. The unstable rf oscillation has a different phase from the linear component, resulting in a beat which shifts to earlier times with increasing power as a result of the larger growth rate. The instability wave form is highly distorted, indicating harmonic generation. After saturation, the rf amplitude begins to fluctuate randomly in time (not shown in Fig. 3).

The density perturbation ($\delta n/n \gtrsim 15\%$) which oc-

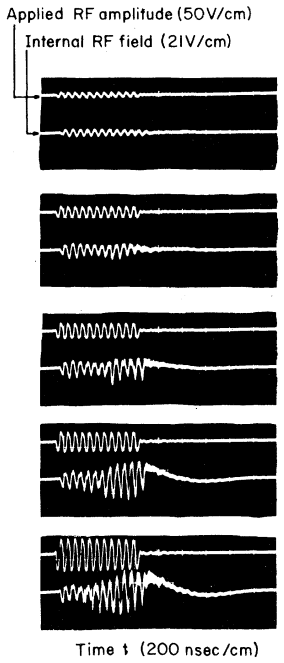

FIG. 3. Temporal plasma response to applied burst at different amplitudes. The lower trace in each picture is the electric field measured by the double T probe located axially in the center of the antenna and radially within the location of maximum density perturbation, i.e., the resonance cone edge. $B_0 = 400$ G, $n_e = 4 \times 10^{10}$ cm^{-3}, $f_0 = 15$ MHz.

curs at the region of the highly peaked rf field shows a similar nonlinear behavior. The density perturbation and large-field region are inclined to the magnetic field at approximately the resonance cone angle. For long rf pulses ($t_{rf} > 1$ μsec) both the density perturbation and the rf field structure break up into several peaks and eventually go over into a turbulent spatial and temporal pattern.

The observed nonlinear phenomena are tentatively explained by the following physical picture. The electron motion in the wave field has two components, an $\vec{E} \times \vec{B}_0$ motion ($\omega \ll \omega_{ce}$) due to the perpendicular electric field component and an axial oscillation due to the parallel electric field component. In spite of the larger perpendicular electric field [$E_\perp \simeq (k_\perp/k_\parallel) E_\parallel \cong 30$ V/cm] the perpendicular $\vec{E} \times \vec{B}_0$ electron velocity and excursion length are smaller than the parallel values. For the parallel electron motion, which is nearly analogous to the field-free situation, we find $v_{\text{oscillatory}}/v_{\text{thermal}} \sim 0.2$ indicating that ponderomotive-force effects, giving rise to drifts in the direction opposite to field intensity gradients, are important.[6] The perpendicular ponderomotive force is smaller by a factor $(\omega/\omega_{ce})^2 \approx 10^{-4}$. The ponderomotive force parallel to $\vec{B}_0$ on the electrons is given by[7]

$$F = -\frac{\partial}{\partial z}\left[\left(\frac{\omega_{pe}}{\omega}\right)^2 \frac{|\partial_z \varphi|^2}{8\pi} + \frac{\omega_{pe}^2}{\omega^2 - \Omega_{ce}^2} \frac{|\partial_x \varphi|^2}{8\pi}\right]. \quad (1)$$

By expelling electrons parallel to $\vec{B}_0$ out of the region of high rf intensity, a positive space-charge imbalance is created which causes ion acceleration. Since the ion Larmor radius ($r_{ci} \sim 1$ cm) is comparable to the cone width ($\Delta r - 0.75$ cm), the ions drift across $\vec{B}_0$. This is consistent with the short time scale ($\Delta t \geq 1$ μsec) on which the perturbation is produced.

In summary, we observe that at large amplitudes the linear wave pattern is modified, and localized, highly peaked fields evolve. Simultaneously, the density profile is altered with density perturbations of $\delta n/n \sim 15\%$ at the regions of the high fields. The density depression and field enhancement appear to reinforce one another since both initially grow exponentially in time.

We gratefully acknowledge valuable discussions with A. Y. Wong, G. Morales, Y. C. Lee, and G. Schmidt. In addition, the technical support by Z. Lucky and M. Lubbers has been invaluable.

*Work supported by the U. S. Energy Research and Development Administration under Contract No. AT (04-3)-34, Project 157.

[1]J. W. Shearer and J. L. Eddleman, Phys. Fluids 16, 1753 (1973).

[2]H. Washimi, J. Phys. Soc. Jpn. 34, 1373 (1973).

[3]R. K. Fisher and R. W. Gould, Phys. Fluids 14, 857 (1971).

[4]W. Gekelman and R. L. Stenzel, Rev. Sci. Instrum. 46, 1386 (1975).

[5]R. L. Stenzel and W. Gekelman, Phys. Rev. A 11, 2057 (1975).

[6]G. Schmidt, *Physics of High Temperature Plasmas* (Academic, New York, 1966).

[7]Y. C. Lee and G. Morales, Phys. Rev. Lett. 35, 930 (1975).

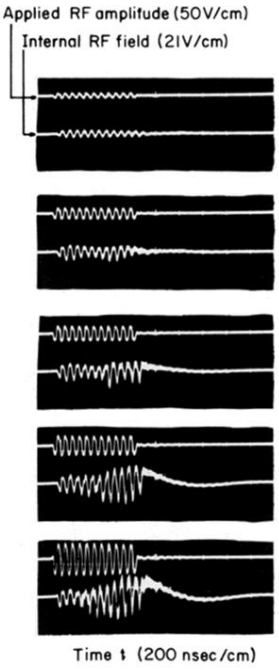

FIG. 3. Temporal plasma response to applied burst at different amplitudes. The lower trace in each picture is the electric field measured by the double T probe located axially in the center of the antenna and radially within the location of maximum density perturbation, i.e., the resonance cone edge. $B_0 = 400$ G, $n_e = 4 \times 10^{10}$ cm^{-3}, $f_0 = 15$ MHz.